

MEASURING CHANGES OF 3D STRUCTURES IN HIGH-RESOLUTION μ CT IMAGES OF TRABECULAR BONE

Norbert Marwan, Jürgen Kurths

Nonlinear Dynamics Group, Institute of Physics, University of Potsdam, 14415 Potsdam, Germany

Peter Saparin

Department of Biomaterials, Max Planck Institute of Colloids and Interfaces, 14424 Potsdam-Golm, Germany

Jesper S. Thomsen

Department of Biology, Institute of Anatomy, University of Aarhus, 8000 Århus, Denmark

Keywords: Measures of complexity, 3D image analysis, structural analysis, trabecular bone, osteoporosis.

Abstract: The appearances of pathological changes of bone can be various. Determination of apparent bone mineral density is commonly used for diagnosing bone pathological conditions. However, in the last years the structural changes of trabecular bone have received more attention because bone densitometry alone cannot explain all variation in bone strength. The rapid progress in high resolution 3D micro Computed Tomography (μ CT) imaging facilitates the development of new 3D measures of complexity for assessing the spatial architecture of trabecular bone. We have developed a novel approach which is based on 3D complexity measures in order to quantify spatial geometrical properties of bone architecture. These measures evaluate different aspects of organization and complexity of trabecular bone, such as complexity of its surface, node complexity, or local surface curvature. In order to quantify the differences in the trabecular bone architecture at different stages of osteoporotic bone loss, the developed complexity measures were applied to 3D data sets acquired by μ CT from human proximal tibiae and lumbar vertebrae. The results obtained by the complexity measures were compared with results provided by static histomorphometry. We have found clear relationships between the proposed measures and different aspects of bone architecture assessed by the histomorphometry.

1 INTRODUCTION

Bone is a dynamic tissue that adapts its architecture to the loading conditions it is subjected to. In addition, from the third decade of life the amount of bone tissue is gradually decreasing. However, in patients with osteopenia or osteoporosis or in astronauts staying in micro-gravity conditions for a long period of time, the bones may change so dramatic that they will lose a significant amount of their stability and the fracture risk increases. These changes may emerge on the one hand as the loss of bone, a decrease of the mineralization of bone, and on the other hand as a change in the micro-architecture of the interior spongy part of the bone called trabecular bone. Structural changes of trabecular bone have received more attention in the last years because the bone loss alone cannot explain all variation in bone strength. Moreover, the rapid progress in high resolution 3D Micro-Computed Tomography (μ CT) imaging facilitates the investigation of the micro-architecture of bone.

The standard method for assessing the bone status and its micro-architecture is bone histomorphometry, which was developed for 2D (Parfitt et al., 1983) and recently extended for 3D analysis (Ito et al., 1998; Hildebrand et al., 1999). More recently developed methods for quantifying the complexity of trabecular structures includes methods using measures of complexity based on symbolic dynamics (Saparin et al., 1998; Saparin et al., 2005), fractal properties (Marwan et al., 2007b) and on recurrence (Marwan et al., 2007a), or using volumetric spatial decompositions (Stauber and Müller, 2006). By applying these approaches to 3D images of trabecular bone, it was shown that the bone micro-architecture changes substantially during the development of osteopenia/osteoporosis. The main conclusions in (Saparin et al., 2005; Marwan et al., 2007a) were that the complexity of the bone micro-architecture decreases with increasing bone loss and that the volume and surface of the trabecular structure changes in a different amount. This latter conclu-

sion confirms former findings that the shapes of the trabeculae change during bone loss, e. g., from plate-like structure to rod-like structure (Hildebrand et al., 1999).

In this study we develop new measures of complexity for quantifying the shape and the complexity of 3D structures. We use 3D geometrical properties like local ratio of bone volume to bone surface and the local configuration of the neighbourhood of the bone voxels. We apply these measures to 3D μ CT images of human proximal tibial and vertebral bodies in order to investigate differences in trabecular bone structure at different stages of bone loss and compare the results with the outcome of the histomorphometrical evaluation of the same bone material.

2 MEASURES OF COMPLEXITY

The idea behind the quantification of a geometrical shape is based on the fact that different 3D objects of the same volume have different surfaces, depending on their geometrical shape. For example, a long cylinder (length is much larger than radius) has a larger surface than a cube of the same volume, and a sphere of the same volume has a smallest possible surface for the same given volume (Fig. 1).



Figure 1: Long cylinder, cube and sphere of same volume ($V = 1000$) have different surface ($S_{\text{cylinder}} = 694$ (for this arbitrary proportion), $S_{\text{cube}} = 600$, $S_{\text{sphere}} = 484$).

Based on the relationship between surface and shape, we introduce measures using the local bone surface and local bone volume. Surface and volume of the trabecular bone are locally estimated in a small cubic box of size s , which moves through the entire 3D image.

Surface and volume could be estimated by a simple *Lego brick* approach. The number of voxels forming the bone structure is used as the volume, and the number of such bone voxels which are connected to the bone marrow (surface voxels) as the bone surface (Fig. 2A). However, this approach is rather problematic, because the amount of surface voxels is actually not a two-dimensional surface measure as it should be, but a three-dimensional volumetric measure. Moreover, the bone volume will be overestimated when such a simple voxel counting algorithm is used. Subsequent calculations based on this surface and volume estimation will lead to even more

erroneous estimations. In order to get more precise results, we apply an *iso-surface* algorithm (Fig. 2B).

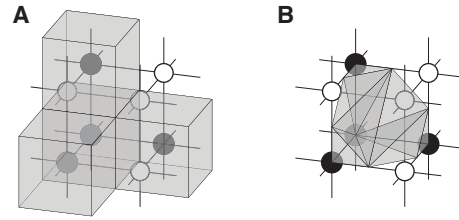


Figure 2: A fragment of data consisting of eight voxels including four bone voxels (black nodes) and four marrow voxels (white nodes). In the *Lego brick* approach (A), the surface of bone is estimated by counting the number of bone voxels which are connected with marrow voxels (the top, front and right black nodes), and the volume is the number of all bone voxels. In the *iso-surface* approach (B), the surface is estimated by the sum of triangles which form an iso-surface between bone and marrow voxels; the volume is the sum of the tetrahedrons which can be filled between such iso-surface and the grid lines. The volume (gray shaded) will be overestimated by using the *Lego brick* approach (A), but will be calculated more precise by using the *iso-surface* approach (B).

An appropriate approach to construct iso-surface is the marching cubes algorithm (Lorenson and Cline, 1987) which is widely used for constructing iso-surfaces in 3D data visualisation. A marching cube (MC) consists of eight neighbouring voxels. If two neighbouring voxels of this MC have voxel value (i. e. one is bone and another is non-bone voxel), the iso-surface will lie between these two voxels. In such MC the iso-surface is formed by a set of triangles, and the surface estimation is the sum of the areas of these triangles (Fig. 2B). Now we introduce the same approach for the estimation of the bone volume. The bone volume within the MC is filled with tetrahedrons in such a way, that the resulting surface equals the iso-surface, which is formed by triangles (Fig. 3). The sum of the volumes of these tetrahedrons is the estimated bone volume contained in the MC.

For the quantification of the 3D shape, we introduce at first the ratio between the local bone surface S_{bone} and the minimal possible surface of the given local bone volume V_{bone} , which is the surface of a sphere S_{sphere} containing this volume V_{bone} . We call this ratio *local shape index* σ_{loc} . Because the local bone volume V_{bone} depends on the size of the moving box s , the normalized local bone volume $\hat{V}_{\text{bone}} = V_{\text{bone}}/s^3$ is used (\hat{V} corresponds to the local bone volume fraction or density BV/TV_{loc}). The local shape index

$$\sigma_{\text{loc}} = \frac{S_{\text{bone}}}{S_{\text{sphere}}} \quad \text{with} \quad S_{\text{sphere}} = \sqrt[3]{36\pi\hat{V}_{\text{bone}}^2} \quad (1)$$

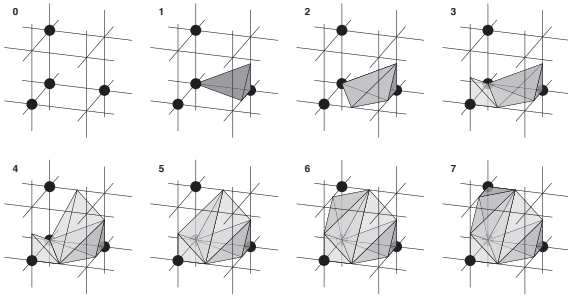


Figure 3: Same fragment as shown in Fig. 2, which is also called marching cube. For volume estimation, the marching cube is filled with tetrahedrons constructed between the iso-surface and the grid lines.

distinguishes between different shapes with the same volume but whose surface differ, like plates and rods. In principle, the value of this index should be equal or larger than one, because the surface of a sphere is the smallest possible surface. However, the object could be cut by the faces of the moving box; these interfaces are not counted for the surface of the structure, resulting in a smaller surface. This can even result in a surface that is smaller than such of a sphere. However, this would mainly be the case if the structure is concave. Therefore, values of σ_{loc} smaller than one represent concave structures, whereas values larger than one represent convex structures.

Because σ_{loc} is computed within a small box while moving through the studied object, we get a frequency distribution of the shape index over the entire object $p(\sigma_{loc})$. Based on this distribution, the *averaged shape index*

$$A_{\sigma} = \langle \sigma_{loc} \rangle_{VOI}, \quad (2)$$

which is the average of all σ_{loc} in the volume of interest (VOI); it measures the mean shape of the trabecular structures.

Next we define the *shape complexity* as the conditional entropy of the joint distribution $p(\sigma_{loc}, V_{loc})$ in a given bone volume V_{loc}

$$C_{\sigma} = - \sum_{\sigma_{loc}, V_{loc}} p(\sigma_{loc}, V_{loc}) \log \frac{p(\sigma_{loc}, V_{loc})}{p(V_{loc})} \quad (3)$$

This measure quantifies the variety of different shapes for various bone volumes. If the bone surface changes in the same manner as the bone volume changes, i. e. the shape of the structure is roughly remaining, this measure will be low. If, however, the shape is changing more dramatically and perhaps irregularly due to changing bone volume, as it is the case for bone loss, C_{σ} will be high.

As already mentioned, an MC is formed from eight neighbouring voxels, arranged in the shape of a cube. The entire VOI is actually a composition of

many such MCs. In each MC, depending on the positions of the bone voxels, there are 256 configurations possible; neglecting rotational and inversion symmetry, there are 15 unique and fundamental MC configurations (Lorensen and Cline, 1987). However, we will only consider rotational symmetry and ignore inversion, hence, we will deal with 21 pseudo-unique MC configurations (Fig. 4). A specific marching cube configuration corresponds to a specific bone surface configuration and, hence, it is related with the complexity of the surface. For all MCs composing the VOI we identify and count each MC configuration and can derive the probability $p(MC)$ with which a certain MC configuration occurs in the 3D architecture.

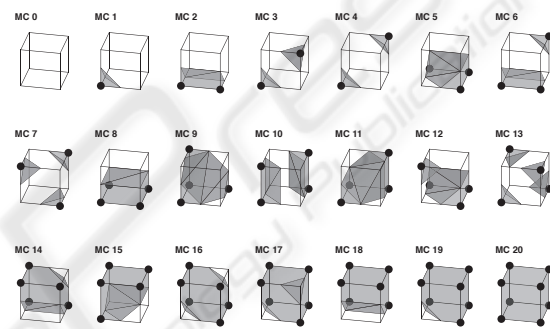


Figure 4: The 21 pseudo-unique marching cube configurations used for defining the *marching cubes entropy index*.

Since these pseudo-unique marching cube configurations (MC cases) are related with the surface complexity, we define an additional measure, the *marching cubes entropy index*

$$I_{MC} = - \sum_{MC} p(MC) \log p(MC) \quad (4)$$

which is the Shannon entropy of the probability density $p(MC)$ of the marching cubes cases; it measures the complexity of the surface of the trabecular structures. Simple complex surfaces will result in low values of I_{MC} , whereas complex surfaces will result in high values of I_{MC} .

Note that shape complexity C_{σ} and marching cubes entropy index I_{MC} characterises different kinds of order in a structure. Whereas I_{MC} assesses a global order (or disorder) of bone surfaces, C_{σ} quantifies the order of certain structural shapes depending on the structure volume. Therefore, these two measures are not necessarily correlated with each other.

3 MATERIALS

These newly introduced measures, Eqs. (2), (3) and (4), are used for the assessment of structural changes

in trabecular bone due to bone loss in osteoporosis.

29 trabecular bone biopsies from proximal tibia bone specimens and 18 entire lumbar vertebral bodies L4 were obtained from the same set of donors. The proximal tibial bone biopsies were scanned at Scanco Medical AG (Bassersdorf, Switzerland) by using a *Scanco μ CT 40* μ CT scanner with a voxel size of $20 \mu\text{m}$ (Thomsen et al., 2005). The vertebral bodies were scanned at Scanco Medical AG by using a *Scanco μ CT 80* with a voxel size of $37 \mu\text{m}$. In order to get comparable images for both skeletal sites, proximal tibia images were downsampled to a voxel size of $40 \mu\text{m}$. The analysed set of specimens includes normal, osteopenic (initial stage of osteoporosis) and osteoporotic bones.

Standardized volumes of interest (VOI) were applied to the μ CT images for quantification of the 3D architecture: The VOI for the proximal tibial biopsies was located 5 mm below the cortical shell and were 10 mm long, whereas the VOI for the vertebra was a $25 \times 15 \times 10 \text{ mm}^3$ cuboid with the center shifted 4.5 mm backwards from the center of the vertebra along its symmetry line (Fig. 5). The structural measures of complexity are then computed using these VOIs. In order to validate the developed measures, the results of the purposed 3D data evaluation were compared against conventional bone histomorphometry (Thomsen et al., 2000). Histomorphometric measures are discussed below.

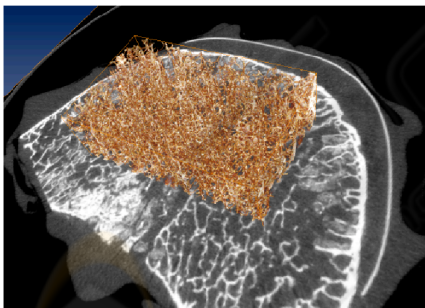


Figure 5: Volume of interest applied to a human lumbar vertebra. Analysed part of the trabecular structure is shown in brown, grey-scale image is the axial CT slice through the middle of the vertebral body.

4 RESULTS

Applying the introduced measures of complexity to the VOIs within the 3D μ CT images, we perform an evaluation of the micro-architecture of the trabecular bone of 29 proximal tibial biopsies and 18 lumbar vertebrae representing different stages of bone loss in os-

teoporosis. The size of the moving box was chosen as $20 \times 20 \times 20$ voxels.

At first we study the differences of the trabecular structure due to bone loss and compare the trabecular bone architecture in proximal tibia and lumbar vertebra (Fig. 6). Bone volume to total volume ratio BV/TV (derived from histomorphometry) characterises the amount of bone material and is used as an indicator of bone loss. We find some remarkable differences between the proximal tibia and the lumbar vertebra.

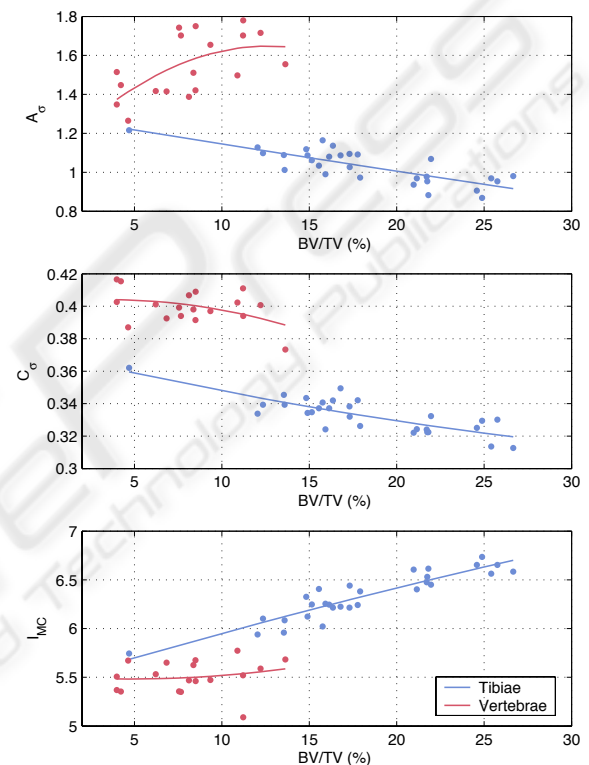


Figure 6: Measures of complexity vs. bone loss (represented by bone volume fraction BV/TV) for proximal tibiae (blue line) and lumbar vertebrae (red line). The lines are square-polynomial fits to guide the eye.

During bone loss, A_σ decreases in the vertebra, but increases in the proximal tibia. Moreover, for high density proximal tibiae ($BV/TV > 20\%$) its values are below one. This suggests that the normal trabecular bone in proximal tibia contains a large number of concave structures. Bone loss causes a shift from concave structures towards convex ones. A_σ for vertebra is higher than one. The Spearman's rank correlation coefficient between BV/TV and A_σ is $R = -0.75$ (proximal tibia) and $R = 0.57$ (vertebra). On a $p = 0.01$ significance level, the correlation for the proximal tibia is significant, but for the vertebrae it is not.

C_σ reveals the same trend for both proximal tibia and vertebra. I_{MC} reveals also the same trend for both skeletal sites. However, the direction of the correlations between C_σ and I_{MC} are opposite. The correlations are only significant for the proximal tibia. From the correlation between I_{MC} and BV/TV we infer that the complexity of the bone surface decreases during bone loss. The anti-correlation with C_σ suggests that the variety of shapes increases during bone loss, as it is the case when plate-like structures deteriorate towards rod-like structures, or rod-like structures become disconnected.

Next, we compare the introduced structural measures of complexity with some of the classical histomorphometrical measures (Tab. 1, Fig. 7). The majority of these measures are significantly correlated to the measures of complexity at the proximal tibia only. This is probably due to a higher variability of the shapes in proximal tibia.

The trabecular separation Tb.Sp measures the mean trabecular plate separation under the assumption that the bone tissue is distributed as parallel plates (Parfitt et al., 1983). At the vertebral body only A_σ is significantly correlated with Tb.Sp. At the proximal tibia both C_σ and I_{MC} are weakly correlated with Tb.Sp.

The nodes-termini ratio Nd/Tm represents the connectivity of the network as it appears on a 2D section (Garrahan et al., 1986). A change in the connectivity of the network causes a change in the complexity of bone surface. Therefore, at the proximal tibia we find that Nd/Tm is strongly correlated with I_{MC} . At the vertebral body Nd/Tm and I_{MC} are also correlated, but this correlation does not reach the level of significance.

A further common way to characterise the trabecular network is the trabecular bone pattern factor TBPf (Hahn et al., 1992). It is, like Nd/Tm, strongly related with the suggested measures of complexity, in particular with I_{MC} . Again, for vertebrae these correlations are not significant.

These results confirm that the averaged shape index A_σ , shape complexity C_σ and marching cubes entropy index I_{MC} express the shape and complexity of the trabecular micro-architecture. The different aspects of the introduced measures of complexity are clearly illustrated at the proximal tibia and by comparing tibia and vertebral trabecular bone architectures. We proved quantitatively that the architecture of the trabecular bone of lumbar vertebra is very different from that of the proximal tibia. This difference is also clearly emphasised by the new structural measures. Therefore, we infer that these measures reveal additional information about the bone structure, which are

Table 1: Spearman's rank correlation coefficients between structural measures of complexity and bone volume fraction as well as histomorphometrical measures. Statistically significant values ($p = 0.01$) are black, non-significant values are gray.

	A_σ	C_σ	I_{MC}
<i>Proximal Tibiae</i>			
BV/TV	-0.75	-0.72	0.88
Tb.Sp	0.45	0.58	-0.64
Nd/Tm	-0.72	-0.65	0.88
TBPf	0.72	0.66	-0.90
<i>Lumbar Vertebrae</i>			
BV/TV	0.57	-0.27	0.25
Tb.Sp	-0.71	0.26	-0.19
Nd/Tm	0.38	-0.07	0.34
TBPf	-0.35	0.14	-0.41

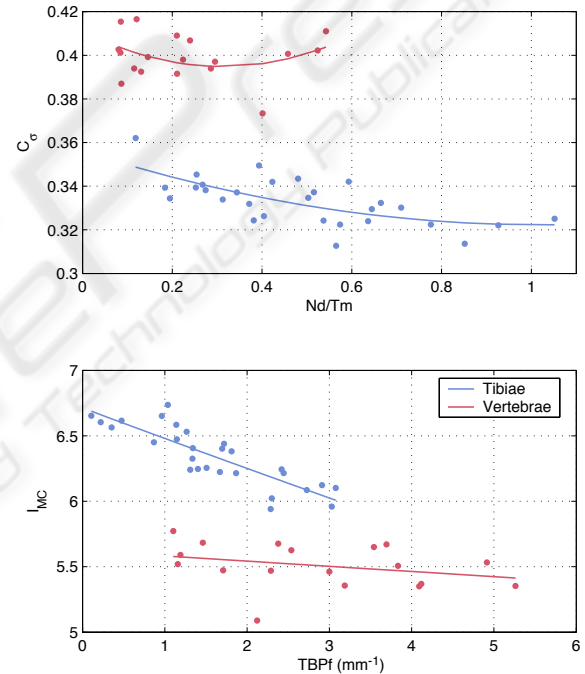


Figure 7: Measures of complexity vs. Nd/Tm and TBPf for proximal tibiae (blue line) and lumbar vertebrae (red line). The lines are squared fits to guide the eye.

not included in BV/TV or any of the histomorphometric measures.

The relationships we found between the developed measures and the bone architecture as well as the relation between the structural complexity measures and the histomorphometric parameters suggest that the proposed new measures of complexity are able to quantify 3D bone architecture. In addition, they contain important information about the trabecular geometry and can be used to describe changes in the spatial structure of trabecular bone.

5 CONCLUSIONS

Using the newly introduced measures, we were able to find significant differences in 3D bone architecture at different levels of bone loss including osteopenia and osteoporosis. We found that the trabecular bone of the proximal tibia contains more concave structures than of lumbar vertebra. The amount of concave structures decreases during bone loss, while the proportion of convex structures increase. Similarly, the complexity of the bone surface is decreasing during bone loss. Although the complexity of the trabecular bone structure is higher in healthy bone, the order of the shapes of local structures depending on its volume is higher in healthy bone. This means that osteoporotic structural elements of a given volume have a higher variability in the shape than healthy bone.

The proposed new structural measures of complexity can be directly computed from 3D images and, thus, are non-invasive and non-destructive. They contain important information about the 3D structure of trabecular bone and can be used to describe the deterioration of the trabecular bone network that takes place during the development of osteopenia and osteoporosis.

ACKNOWLEDGEMENTS

This study was made possible in part by grants from the Microgravity Application Program/ Biotechnology from the Human Spaceflight Program of the European Space Agency (ESA) and support from Siemens AG and Scanco Medical AG. Scanco Medical AG is gratefully acknowledged for μ CT scanning the bone samples. Erika May and Wolfgang Gowin, Carité Berlin, Campus Benjamin Franklin, are gratefully acknowledged for preparing the bone samples. Inger Vang Magnussen, University of Aarhus, is acknowledged for help preparing the bone samples for histomorphometry.

REFERENCES

- Garrahan, N. J., Mellish, R. W. E., and Compston, J. E. A. (1986). A new method for the two-dimensional analysis of bone structure in human iliac crest biopsies. *Journal of Microscopy*, 142:341–349.
- Hahn, M., Vogel, M., Pompesius-Kempa, M., and Delling, G. (1992). Trabecular bone pattern factor – a new parameter for simple quantification of bone microarchitecture. *Bone*, 13:327–330.
- Hildebrand, T., Laib, A., Müller, R., Dequeker, J., and Rüeggsegger, P. (1999). Direct Three-Dimensional Morphometric Analysis of Human Cancellous Bone: Microstructural Data from Spine, Femur, Iliac Crest, and Calcaneus. *Journal of Bone and Mineral Research*, 14:1167–1174.
- Ito, M., Nakamura, T., Matsumoto, T., Tsurusaki, K., and Hayashi, K. (1998). Analysis of trabecular microarchitecture of human iliac bone using microcomputed tomography in patients with hip arthrosis with or without vertebral fracture. *Bone*, 23(2):163–169.
- Lorensen, W. E. and Cline, H. E. (1987). Marching cubes: A high resolution 3d surface construction algorithm. *SIGGRAPH Comput. Graph.*, 21(4):163–169.
- Marwan, N., Kurths, J., and Sapanin, P. (2007a). Generalised Recurrence Plot Analysis for Spatial Data. *Physics Letters A*, 360(4–5):545–551.
- Marwan, N., Sapanin, P., and Kurths, J. (2007b). Measures of complexity for 3D image analysis of trabecular bone. *The European Physical Journal – Special Topics*, 143(1):109–116.
- Parfitt, A. M., Mathews, C. H. E., Villanueva, A. R., Kleerekoper, M., Frame, B., and Rao, D. S. (1983). Relationships between Surface, Volume, and Thickness of Iliac Trabecular Bone in Aging and in Osteoporosis. *Journal of Clinical Investigation*, 72:1396–1409.
- Sapanin, P. I., Gowin, W., Kurths, J., and Felsenberg, D. (1998). Quantification of cancellous bone structure using symbolic dynamics and measures of complexity. *Physical Review E*, 58(5):6449.
- Sapanin, P. I., Thomsen, J. S., Prohaska, S., Zaikin, A., Kurths, J., Hege, H.-C., and Gowin, W. (2005). Quantification of spatial structure of human proximal tibial bone biopsies using 3D measures of complexity. *Acta Astronautica*, 56(9–12):820–830.
- Stauber, M. and Müller, R. (2006). Volumetric spatial decomposition of trabecular bone into rods and plates – A new method for local bone morphometry. *Bone*, 38:475–484.
- Thomsen, J. S., Ebbesen, E. N., and Mosekilde, L. (2000). A New Method of Comprehensive Static Histomorphometry Applied on Human Lumbar Vertebral Cancellous Bone. *Bone*, 27(1):129–138.
- Thomsen, J. S., Laib, A., Koller, B., Prohaska, S., Mosekilde, L., and Gowin, W. (2005). Stereological measures of trabecular bone structure: comparison of 3D micro computed tomography with 2D histological sections in human proximal tibial bone biopsies. *Journal of Microscopy*, 218(2):171–179.